An Anatomically Accurate Finite Element Brain Model: Development, Validation and Comparison to Existing Models

L. E. Miller[1,2], J. E. Urban[1,2], and J. D. Stitzel[1,2]
[1]Wake Forest School of Medicine; [2]Virginia Tech-Wake Forest University Center for Injury Biomechanics

ABSTRACT

The objective of this study was two-fold. The first objective was to develop and validate a high resolution, anatomically accurate brain finite element (FE) model from the International Consortium for Brain Mapping (ICBM) brain atlas using a voxel-based mesh generation approach. The second objective was to quantitatively compare performance of six validated brain FE models in three validation conditions against localized brain motion data. The ABM was developed from the ICBM brain atlas by converting each voxel into an element using a custom code developed in MATLAB (Mazziotta et al. 1995, 2001). The brain material properties were optimized using a Latin hypercube design (LHD) method. The ABM was validated against three experimental cadaver tests conducted by Hardy et al. (2001; 2007) through FE simulation in LS-DYNA. The three experimental tests considered for validation were: C755-T2 (occipital impact), C383-T1 (frontal impact), and C291-T1 (parietal impact) (Hardy et al. 2001; Hardy 2007). The five additional FE models considered in the current study are the Simulated Injury Monitor (SIMon), the Global Human Body Models Consortium (GHBMC) head model, the Total Human Model for Safety (THUMS) head model, the Kungliga Tekniska Högskolan (KTH) model, and the Dartmouth Head Injury Model (DHIM) (Kleiven and von Holst 2002; Takhounts et al. 2003; Kimpara et al. 2006; Kleiven 2007; Mao et al. 2013; Ji et al. 2014a). Validation results for the SIMon, GHBMC, and THUMS models were also obtained through direct simulation in LS-DYNA. Results for the remaining models were obtained from published literature. To evaluate model performance, the error between experimental and predicted displacements was quantified using a relatively new metric called CORA (CORrelation and Analysis) (Gehre et al. 2009). The ABM shows good agreement with experimental validation data. Additionally, looking at each model's average CORA score between the three impacts, the ABM scores the best CORA rating. This result indicates that of the models considered, the ABM demonstrates the strongest ability to predict local brain deformations under a range of impact severities and directions.

INTRODUCTION

Each year, approximately 1.7 million people in the United States suffer from traumatic brain injury (TBI) (Faul et al. 2010). TBI is a major public health concern as it is a leading cause of disability and injury-related death - accounting for nearly one third of all injury-related deaths (Coronado et al. 2011). To prevent and treat these types of injuries, the fundamental injury

mechanisms need to be well-characterized and understood. There are various theories about what causes brain injury, such as the development of positive and negative pressure in coup and contrecoup injuries, rotational effects, and relative motion between the brain and skull (Holbourn 1943; Pudenz and Shelden 1946; Gross 1958; Hodgson et al. 1969). While each of these mechanisms has been shown to induce injury, there is still a great deal that we do not know about the fundamentals of brain injury and injury thresholds. Various methods have been used over the years to investigate and gain a deeper understanding of brain injury mechanisms, including animal tests, cadaver studies, anthropomorphic test devices (ATDs), and computational model (Takhounts et al. 2003). Finite element (FE) models are powerful tools because they provide spatial and temporal distributions of stresses and strains throughout the brain. The quality of a model's predictions, however, is dependent on the accuracy of the modeled geometry and the model's ability to describe complex mechanical behavior and material response.

Models with varying degrees of anatomical accuracy and complexity have been developed over the last several decades. Anatomical accuracy of the models varies with the number of elements, ranging from models employing a rather coarse mesh and containing approximately 20,000 elements to more accurate models containing almost two million elements. As the number of elements increases, however, computational costs also increase; therefore, for some applications, the decrease in anatomic detail is an accepted tradeoff for reduced computation time. The constitutive models employed for brain tissue vary across FE models and include linear and quasi-linear viscoelastic, hyperelastic, and fully nonlinear Green-Rivlin models. There is also a wide range of material properties and parameters used throughout the literature. Reported values for shear relaxation moduli, for example, span orders of magnitude (Chatelin et al. 2010). Finally, models differ in their approach to representing the boundary condition at the brain-skull interface. Some models directly couple the brain and skull, which allows no motion between the brain and skull, while others simulate relative brain-skull motion through a 'soft' CSF layer or various sliding contact algorithms.

Once an FE model has been developed, it must be validated against experimental data before it can reliable be used to predict response and injury. Brain models are commonly validated against experimental pressure response and localized brain motion data. Specifically, the cadaver experiments conducted by Nahum et al. (1977) and the long-duration impact experiment conducted by Trosseille (1992) are used to assess the intracranial pressure (ICP) response, whereas the set of cadaver impact experiments conducted by Hardy et al. (2001; 2007) is used to validate the local brain displacements. Models should be validated against relative displacements as well as ICP data, as it has been shown that predicting the correct pressure response does not necessarily predict the correct strain (Kleiven and Hardy 2002; Hardy 2007). The finding that some brain injuries (e.g., diffuse axonal injury) are dependent on strain reinforces the importance of validating models with displacement data as well as pressure data (Tse et al. 2014). This motivates validation using the more robust displacement data set that represents the strain field throughout the brain, which will be used in the current study. While there are some experiments that are commonly used by researchers for model validation purposes, there is no standard for all brain FE models and it is difficult to compare results between models. Thus, there is a need for a metric that allows quantitative comparisons of model performance and a robust method for objectively rating model validation results.

A recent study illustrates the need for a standardized performance metric and rating method for validation results (Deck and Willinger 2009). This study presented validation results for six brain models for three localized brain motion cadaver experiments. One limitation of this

work is that the models were not labeled, so the reader does not know which model performed best in any given validation condition. Additionally, the study considered only the first 50 ms of the response, which is a substantial omission considering the duration of one of the impacts examined was 120 ms. Furthermore, the study examined a reduced set of measured responses, excluding a large amount of validation data. For one experiment, only 2 of 36 (5.6%) responses were analyzed. Finally, the investigation quantitatively compared model performance using two error methods: the normalized integral square error (NISE) and Russel's error measures (RUS), which both evaluate phase and magnitude error to determine a comprehensive metric describing the difference in two curves (Jovanovski 1981; Donnelly et al. 1983). A limitation to this type of error analysis is that a high rating could indicate a large phase shift rather than good fit to the experimental data. These calculations are also sensitive to noise and filtering.

The objective of this study was two-fold. The first objective was to develop and validate a high resolution, anatomically accurate brain finite element (FE) model from the International Consortium for Brain Mapping (ICBM) brain atlas using a voxel-based mesh generation approach. The second objective was to quantitatively compare performance of six validated brain FE models in three validation conditions against localized brain motion data. The three experimental impact tests used for validation are: C755-T2 (occipital impact), C383-T1 (frontal impact), and C291-T1 (parietal impact) (Hardy et al. 2001; Hardy 2007). The additional models considered are the Simulated Injury Monitor (SIMon), Global Human Body Models Consortium (GHBMC) head model, Total Human Model for Safety (THUMS) head model, Kungliga Tekniska Högskolan (KTH) model, and the Dartmouth Head Injury Model (DHIM) (Kleiven and von Holst 2002; Takhounts et al. 2003; Kimpara et al. 2006; Kleiven 2007; Mao et al. 2013; Ji et al. 2014a). Model performance was evaluated using a relatively new metric called CORA (CORrelation and Analysis) (Gehre et al. 2009). The CORA method presents an improvement over existing error analysis methods by combining two independent sub-methods, which compensates for the weaknesses of either method alone.

METHODS

ABM Development

The ABM was developed from the geometry of the ICBM brain template, a high-resolution structural average of T1-weighted MRI scans of normal young adult brains. The ICBM average brain template is a probabilistic atlas in Montreal Neurologic Institute (MNI) space that represents that average anatomy of a normal adult brain, while the template is derived from Talairach and Tournoux atlas space (Mazziotta et al. 1995, 2001). An FE model was created from this image set by converting each 1mm isotropic voxel into a single element of the same size using a custom code developed in MATLAB (The MathWorks, Natick, MA). While the high level of detail provided by the atlas allows the opportunity to represent many detailed brain structures, initial model development combined the label maps to include only four distinct parts: cerebrum (combined white and gray matter), cerebellum, CSF, and ventricles. The falx cerebri and tentorium cerebelli are important structures in the cranium which were not represented in the ICBM atlas, so they were manually implemented into the model. The falx was defined as a layer of shell elements along the midsagittal plane, and the tentorium as a layer of shell elements on the superior surface of the cerebellum, separating the cerebrum and cerebellum (Figure 1b). Lastly, a layer of rigid shells surrounding the external surface of the CSF was

generated in LS-PrePost to completely enclose the model. The current model, shown in Figure 1, has approximately 2 million nodes and elements.

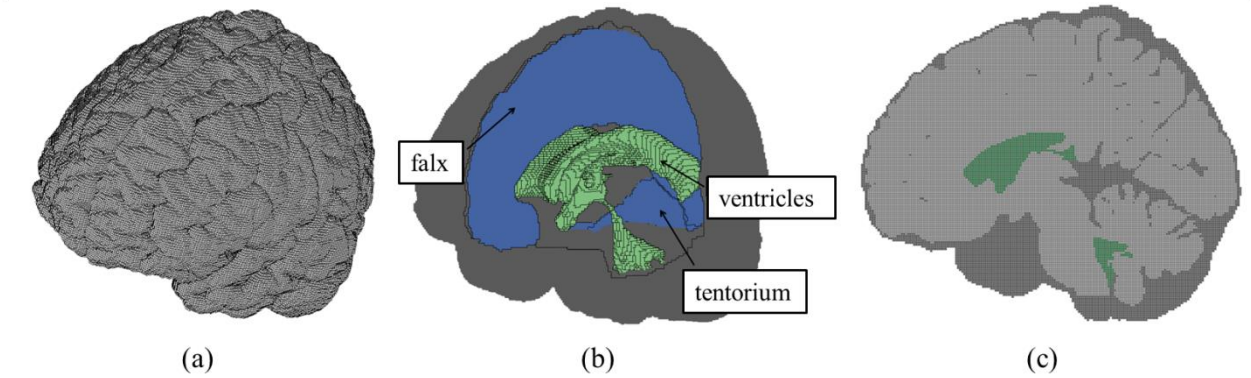

Figure 1: Isometric view of the ABM showing detail of sulci and gyri (a), view inside the skull showing the falx, tentorium and ventricles (b), and a sagittal cross section of the ABM (c).

The treatment of interface conditions and the selection of material models and parameters are very important aspects of any FE model. The boundary condition at the brain-skull interface is particularly important because relative motion between the brain and skull is necessary to accurately model the response of the brain. The ABM preserves relative motion at the brain-skull interface by modeling the CSF as a fluid-like material which allows large element deformations to simulate relative motion. This implementation was motivated by the results of an investigation conducted by Chafi et al. (2009) that evaluated the effects of three different CSF constitutive models: elastic fluid, viscoelastic, and nearly incompressible elastic. This study found that the most comparable results to experimental data resulted from modeling the CSF as a fluid-like material (Chafi et al. 2009).

Brain Material Optimization. The values of brain material parameters vary greatly throughout the literature, which motivates the current optimization study. Brain tissue is often modeled using a linear viscoelastic material formulation (Al-Bsharat et al. 1999; Zhang et al. 2001b; Takhounts et al. 2003; Horgan and Gilchrist 2004; Jiroušek et al. 2005; Kimpara et al. 2006; Mao et al. 2013). The shear relaxation behavior is described by:

$$G(t) = G_\infty + (G_0 - G_\infty) * e^{-\beta t} \quad (1)$$

where G_∞ is the infinite shear modulus, G_0 is the initial shear modulus, and β is the decay constant. Therefore, this material model was selected for material optimization. Brain density (ρ), bulk modulus (K), and the three shear parameters (G_∞, G_0, β) were varied using Latin hypercube sampling (LHS) to generate 100 combinations of material parameters, or 100 distinct brain material models. In LHS, each parameter is varied over a predefined range independent of the values of other variables and orthogonal sampling is employed over the multidimensional sample space to generate samples that are representative of total variability. Brain material parameters were selected from the LHS to optimize performance in three experimental conditions. Detailed discussion of the material optimization is provided in Miller et al. (2016).

Validation against Localized Brain Displacements

Model validation results against relative displacement data for six FE brain models will be presented and quantitatively compared. Relative displacement data from the following three cadaver impact experiments, provided by Hardy et al. (2001, 2007), will be considered: C755-T2

(occipital impact), C383-T1 (frontal impact), and C291-T1 (parietal impact). These three tests were selected because they vary in impact direction (frontal, occipital, parietal) and magnitude (Table 1). Additionally, these three tests are commonly used to validate head models, so it will be beneficial to future model development to have a standard method to quantify performance for comparison to existing models (Zhang et al. 2001a; King et al. 2003; Kimpara et al. 2006; Kleiven 2006; Mao et al. 2006; Takhounts et al. 2008; Ji et al. 2014c).

Local displacements at various locations within the brain were measured during the cadaver impact experiments using implanted radio-opaque neutral density targets (NDTs) and a high-speed biplanar X-ray system to track their relative motion. For the three experiments considered, NDTs were implanted in the cadaver brain in 2-3 vertical columns. Three-dimensional skull kinematics were evaluated with an accelerometer array affixed to the cadaver skull and used to determine linear and angular velocities at the head center of gravity (CG) (Hardy et al. 2001).

Results for the ABM, SIMon, GHBMC, and THUMS models were obtained through simulation in LS-DYNA (MPP, Version 971, R6.1.1, LSTC, Livermore, CA) by applying the CG velocity curves to the skull. To compare relative displacements in the FE models to the experimental data, nodes closest to the physical location of each NDT were identified for each test configuration and local displacements at these nodes were calculated throughout the simulation. For the KTH and DHIM models, validation results available in the literature were digitized for comparison.

Table 1: Summary of Experimental Validation Conditions

	Hardy C755-T2	Hardy C383-T1	Hardy C291-T1
	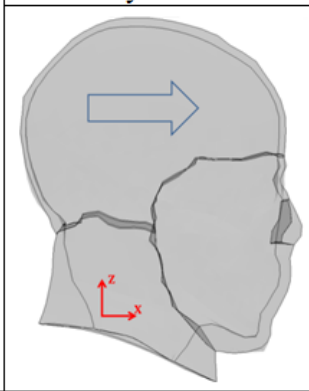	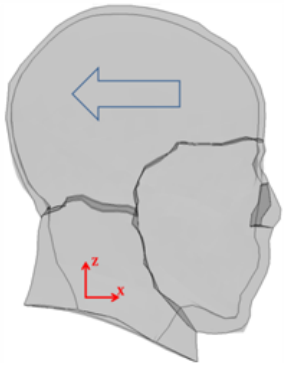	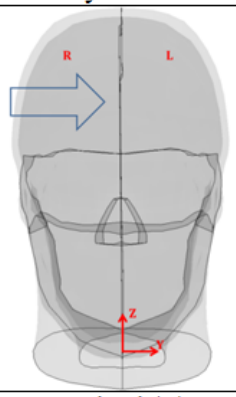
Impact location	occipital	frontal	parietal (R)
Impact type	acceleration	deceleration	deceleration
Relative severity	low	medium	high
Peak G (g)	22	63	162
Delta V (m/s)	1.90	3.91	4.47
Impact Duration (ms)	59	118	98
NDTs	two columns of five	two columns of six	three columns of five*

*results for all NDTs in this experimental test were not reported due to NDT tracking difficulties in the original source paper (Hardy 2007)

Model Performance. To evaluate model performance, error between experimental and predicted displacements was quantified using a metric called CORA (CORrelation and Analysis), a relatively new metric developed to assess FE model performance (Gehre et al. 2009). Historically, FE model performance has been evaluated through comparison of peak

values or through various point-by-point error analysis methods (Yu et al. 2004). In contrast, CORA is an objective rating method that evaluates the similarity of two curves using two independent sub-rating methods: a corridor method and a cross correlation method. In an evaluation of objective rating methods, Vavalle et al. (2013) found CORA to be the most comprehensive metric of the three objective rating methods studied (Sprague and Geers, Cumulative Standard Deviation, and CORA). These methods each produce a rating that ranges from 0 to 1, which are then averaged to determine the overall CORA rating (1 indicates a perfect match). The sub-methods are used in combination because it has been found that they compensate for the disadvantages of either method alone (Gehre et al. 2009). Previous methods used to assess model performance are not as strong as CORA because they typically either only look at peak values or use a point-by-point comparison, such as root-mean-square (RMS), to quantify error. In addition to incorporating both point-by-point and peak value comparisons for assessing model performance, CORA is also able to evaluate the cross correlation of two curves.

Brain FE Model Description and Comparison

Brief descriptions of the five additional validated brain FE models (Figure 2) considered in the current study are provided below. See Appendix for more detailed descriptions of material models.

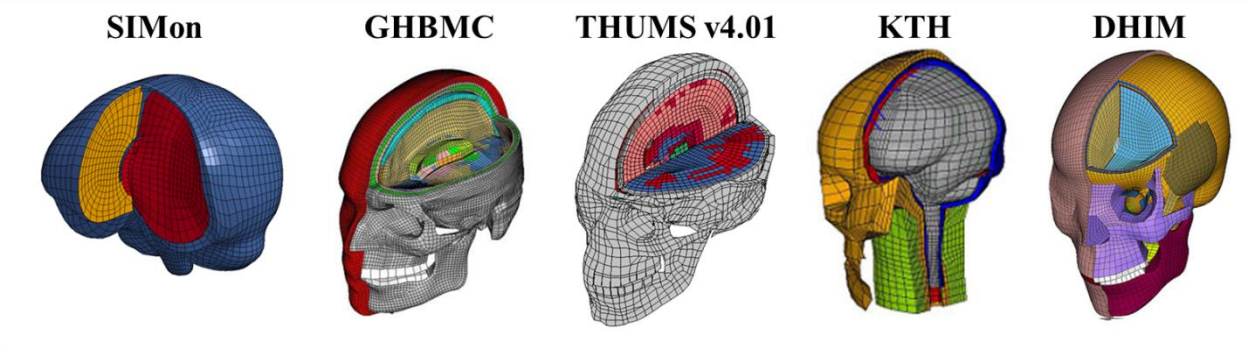

Figure 2: Additional five validated brain FE models considered in the current study.

Simulated Injury Monitor (SIMon). The SIMon model was proposed in 2003 (Takhounts et al. 2003) and employs simple geometry to achieve very short run times. It was based on the model originally developed by DiMasi et al. (1995) and later improved by Bandak and Eppinger (1994) and Bandak et al. (2001). The model includes a rigid skull, CSF, cerebrum, cerebellum, brain stem, ventricles, bridging veins and a falx and tentorium and a Kelvin-Maxwell viscoelastic material model is used to model brain tissue (Figure 2).

Global Human Body Models Consortium (GHBMC). The GHBMC head model was meshed from a Computer Aided Design (CAD) dataset developed from MRI and CT scans of an average adult male. The set included geometry representing skin surface, skull and facial bones, sinuses, cerebrum, cerebellum, lateral ventricles, corpus callosum, thalamus, and brainstem (Figure 2). Geometry for cerebral white matter was also used to develop white matter meshes. Aspects of the anatomy not included in the CAD dataset but that were implemented into the model include the falx and tentorium, bridging veins, and the meningeal layers (pia, arachnoid, dura). Kelvin-Maxwell viscoelastic model was used to model the gray and white matter.

Total Human Model for Safety (THUMS). The basic geometry of the brain model of the Total Human Model for Safety (THUMS) Version 4 (THUMS AM50 Ver 4, Toyota TCRDL,

Japan) was obtained from a male data set available in the Visible Human Project (NIH, USA) and was created according to anatomical references (Kimpara et al. 2006). The basic anthropometry of the skull was obtained from a commercial data package (Viewpoint Datalabs, USA) and then modified based on anatomical references (Clemente 1985). The THUMS head model consists of the skull and facial bones, cerebrum (distinct white and gray matter), cerebellum, brainstem, CSF, meningeal membranes, falx cerebri, tentorium cerebelli, and the sagittal sinus (Figure 2). A linear viscoelastic material model was used to model the response of the gray and white matter.

Kungliga Tekniska Högskolan (KTH). Kleiven and Hardy proposed an FE model of the human head in 2002 known as the Kungliga Tekniska Högskolan (KTH) FE model (Kleiven and von Holst 2002). This model includes the scalp, skull, cerebrum, cerebellum, meninges, CSF, bridging veins, and a simplified neck (Figure 2). In 2006, the model was validated against two pressure experiments and the C755-T2, C383-T1, and C291-T1 displacement experiments (Kleiven 2006). Full displacement-time histories for most NDTs are provided by Kleiven (2006), so this data was digitized for comparison. The KTH model presented in Kleiven (2006) modeled brain tissue with a hyperelastic Mooney-Rivlin constitutive model combined with a linear viscoelastic model to account for rate effects. The Mooney-Rivlin and shear constants used in this model are based on those derived by Mendis et al. (1995), but scaled corresponding to an effective (long-term) modulus of 520 Pa. The most commonly cited version of the KTH model, described in Kleiven (2007), uses an Ogden model to characterize brain tissue. Validation results for the displacement experiments are not presented in Kleiven (2007), but can be found in Giordano and Kleiven (2014). Displacement results for the Ogden model were digitized for the C755-T2, C383-T1, and C291-T1 experiments, although it should be noted that only the first 50 ms are presented for each case. The results of the KTH model using both the Mooney-Rivlin and Ogden material models are examined in the current study.

Dartmouth Head Injury Model (DHIM). The Dartmouth Head Injury Model (DHIM) was created from a high-resolution T1-weighted MRI of an athlete clinically diagnosed with concussion (Ji et al. 2014b). The model features a skull, facial bones, cerebrum (combined white and gray matter), cerebellum, brainstem, corpus callosum, meningeal layers, CSF, ventricles, falx cerebri and tentorium cerebelli (Figure 2). An Ogden hyperelastic material model identical to the 'average' model reported by Kleiven (2007) is employed for brain tissue, in addition to a six-term Prony series characterizing viscoelasticity. NDT displacements were digitized for the C755-T2 and C383-T1 cases (Ji et al. 2014c). It is important to note that only the 'corner' NDTs were reported for both cases (4 NDTs each) – that is, the highest and lowest NDT in the anterior and posterior columns. Results for the C291-T1 parietal impact were not found in the literature.

RESULTS

ABM Material Properties

By comparing material parameters and model performance, it was found that the shear parameter, G_0, has the largest influence on model response (Figure 3). This analysis was also used to determine optimal values for the five brain material parameters from the LHS (indicated with a red star in Figure 3). The parameters were found to be: ρ = 1,123 kg/m^3, K = 0.1069 GPa, G_0 = 5.16 kPa, G_∞ = 1.86 kPa, β = 67.58 s^{-1}.

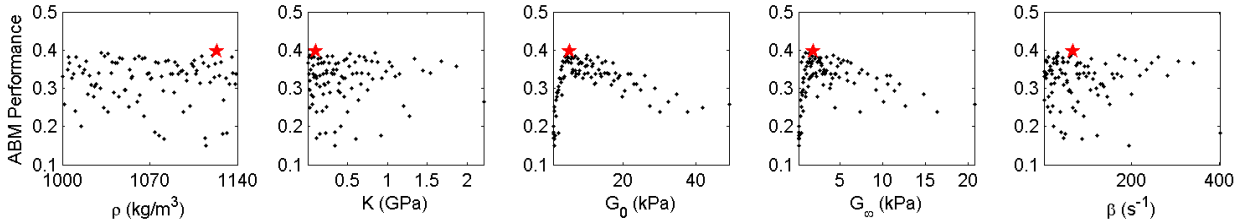

Figure 3: Relationships between model performance and brain material parameters.

Validation Results

Simulated displacements at each NDT location are compared to the experimental displacements in the two in-plane directions. For the occipital impact, displacements are evaluated in the x- and z-directions at each of the 10 NDT locations. This results in a total of 20 CORA scores for each model in the C755-T2 occipital impact. CORA scores for each of the models considered are shown in Figure 4 by NDT location.

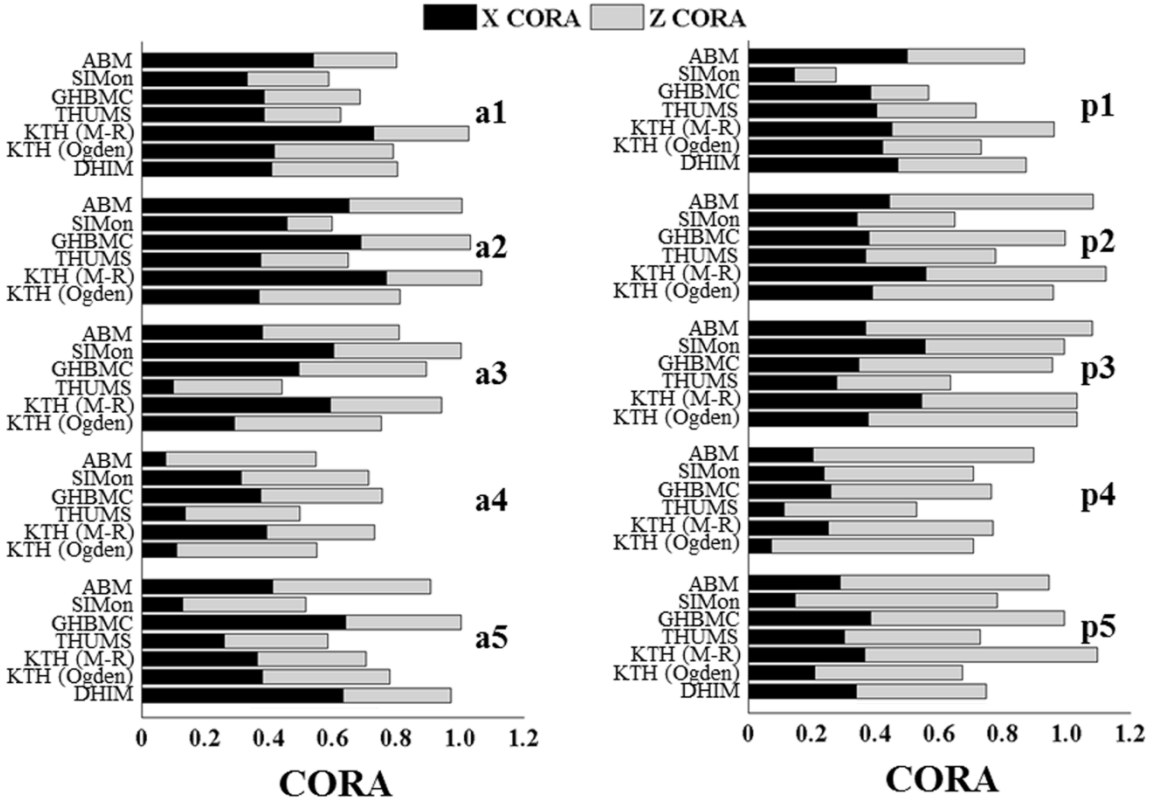

Figure 4: X and Z CORA scores for the 10 NDTs in the occipital (C755-T2) impact.

Once again for the frontal impact, displacements are evaluated in the x- and z-directions. For this case, however, there were 12 implanted NDTs, resulting in 24 possible CORA scores per model. These scores for each model are displayed by NDT location in Figure 5.

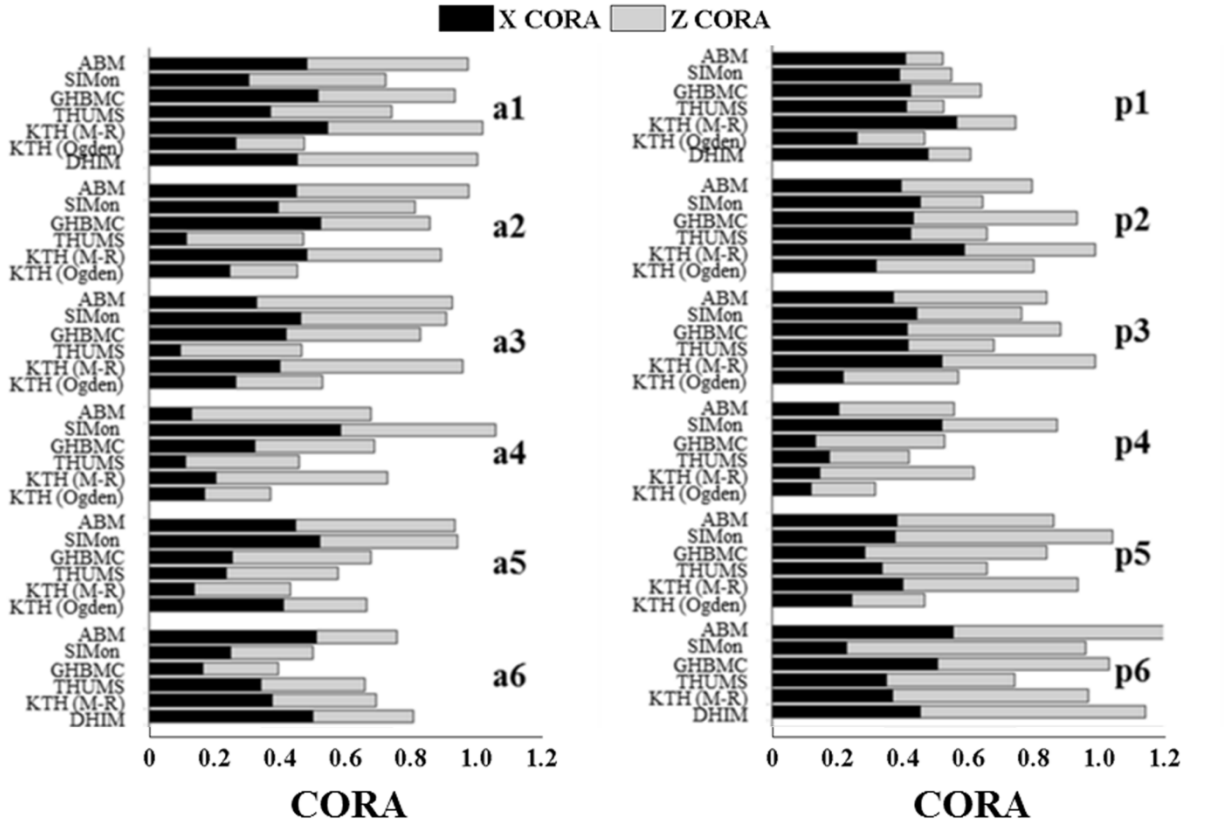

Figure 5: X and Z CORA scores for the 12 NDTs in the frontal (C383-T1) impact.

For the parietal impact, displacements are evaluated in the y- and z-directions. There were three implanted NDT columns in this experiment (2 in the left hemisphere and 1 in the right hemisphere), as opposed to 2 columns each in the previous two experiments. This results in a larger number of implanted NDTs (total of 15). Results were not reported for all 15, however, so there simulated displacements were compared to experimental displacements at the 12 reported NDT locations. The CORA scores for each model are displayed in Figure 6.

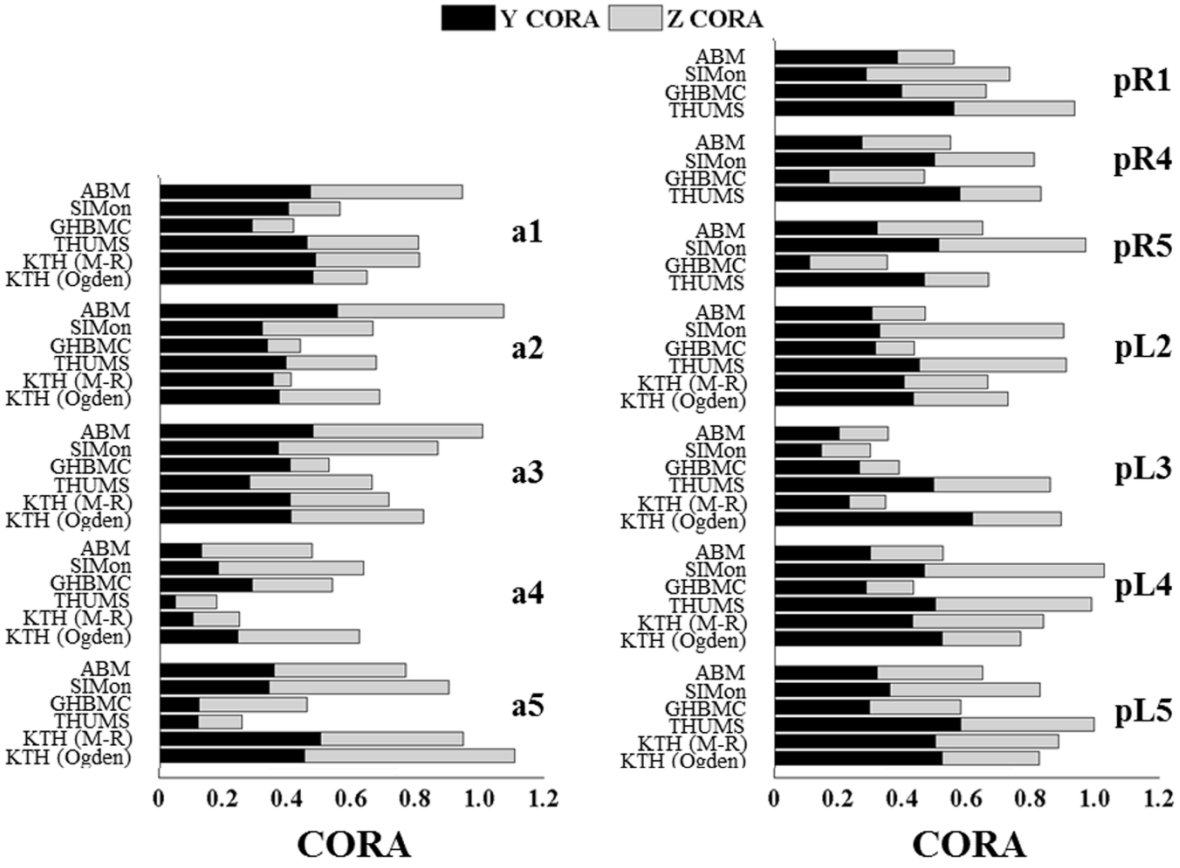

Figure 6: Y and Z CORA scores for the 12 NDTs in the parietal (C291-T1) impact.

Additionally, by combining the ratings for each NDT, average CORA scores were computed for each model (Table 3). Another way of comparing performance between models is to look at the rank in each impact condition. Table 3 also shows the rank and average rank for each model.

Table 2: CORA scores for each model in the 3 experimental configurations

	C755-T2	C383-T1	C291-T1	Average	Std. Dev.	Rank	Ave. Rank
ABM	0.448	0.420	0.338	**0.402**	0.0572	**2, 2, 4**	**2.67**
SIMon	0.341	0.412	0.388	0.380	**0.0361**	5, 3, 2	3.33
GHBMC	0.432	0.386	0.240	0.353	0.100	3, 4, 6	4.33
THUMS v4	0.309	0.295	0.370	0.325	0.0399	7, 6, 3	5.33
KTH (M-R)	**0.473**	0.368	0.330+	0.390	0.0741	1, 5, 5	3.67
KTH (Ogden)*	0.390	0.257	**0.399+**	0.349	0.0795	4, 7, 1	4.00
DHIM**	0.316	**0.432**	--	0.374	0.082	6, 1, -	3.50

+only includes left column of NDTs
*only includes first 50 ms of response
**only includes results for 4 'corner' NDTs

DISCUSSION

C755-T2 Occipital Impact

For the occipital impact, the models examined in the current study display similar overall characteristics when compared to each other, as well as to the experimental data. In most cases, the models achieve good CORA scores, indicating good performance. The plots of CORA scores in the x- and z-directions at each NDT (Figure 4) reveal patterns displayed by several models. For example, in the inferior nodes of the anterior column (a1-a3), most models perform better in the x-direction (score higher X CORA than Z CORA), and perform better in the z-direction for the superior nodes of the posterior column (p2-p5). Additionally, we see that performance at the a4 NDT was relatively low for all of the models, while the models did consistently well in the x- and z-directions at p2 and p3. The models that consistently performed the best in this configuration were the ABM, GHBMC, and KTH models.

C383-T1 Frontal Impact

The frontal impact experiment was longer in duration (118 ms) than the occipital impact (64 ms). This increase in response time results in more complex displacement signals and, in general, somewhat lower CORA ratings. Several models are able to capture the overall experimental behavior and magnitude of displacement for numerous NDTs. This is confirmed by high CORA scores in Figure 5; in particular, good overall response at a specific location can be assumed when good CORA scores are consistent in the x- and z-directions. This behavior is exhibited by many models at NDTs a1, p3 and p6. In contrast, there appear to be locations where the models are able to predict response well in one direction, but not the other. For example, at a6 and p1, most models attain a significantly higher CORA rating in the x-direction than in the z-direction; at p5 we see the opposite behavior. All models perform relatively well in this impact configuration, with the DHIM, ABM, and SIMon models achieving the highest overall CORA scores.

C291-T1 Parietal Impact

The final impact simulated in the current study was the C291-T1 parietal impact, which was the most severe with a maximum head acceleration of 162 g's. This experiment was initialized with three columns of NDTs - an anterior and posterior column in the left hemisphere of the brain (opposite to impact site), and a posterior column in the right hemisphere (at impact site). Two NDTs in the right column and 1 NDT in the left posterior column were omitted from the published experimental data, which may be attributed to the severity of the impact. For this reason, the results for the right NDT column are frequently omitted in published model validation studies, so we are only able to compare results in this column for the four models simulated in the current study (ABM, SIMon, GHBMC, and THUMS). Although these responses are typically difficult to match, the THUMS model does very well in predicting the y response for the right posterior column. This is likely because the THUMS brain is slightly stiffer than the other models, so it is able to constrain lateral motion better than the other models. This same quality, however, is responsible for the poor performance of the THUMS model in the anterior column, where the model under predicts the experimental displacement. The models that performed the best in this configuration were the ABM, KTH, and SIMon models.

Overall Performance

In the occipital condition, all models perform relatively well, with the KTH model (with Mooney-Rivlin material model) scoring the highest CORA rating of 0.473. Of the models considered, most achieved the best CORA rating in this configuration, which is likely because this impact was the lowest severity with the shortest response time. In the C383-T1 impact, the DHIM had the highest CORA score of 0.432. It should be noted, however, that this rating was based on the response of only 4 of the 12 total NDTs, so it may not be representative of the overall response of the DHIM. Considering the remaining models whose performance was based on the response of all 12 NDTs, the ABM perform best with a CORA scores of 0.420. The KTH model (with Ogden material model) scored the best CORA score (0.399) in the parietal impact. Looking at each model's average CORA score between the three impacts, the ABM has the best average rating. Another way to compare the performance of the models that is not sensitive to higher scores in one condition relative to another, is to rank the models from best to worst and consider their relative performance. This was done for the three impact configurations (Table 3) and the result indicates that the ABM has the best rank. Quantitative comparison of model performance was conducted using CORA, which is proposed as the best method for evaluating and comparing validation performance between models. The results of this comparison indicate that different models perform better under different experimental conditions and several models consistently perform better than the others, including ABM and KTH models.

CONCLUSIONS

Well-validated brain FE models are powerful tools for studying brain injury and improve our ability to prevent and mitigate TBI. As new brain models, objective rating and comparison are vital so model performance under validation conditions can be consistently analyzed. Validation against additional displacement tests should be conducted in the future as well as validation using data from magnetic resonance elastography (MRE) studies that measure strain data in live humans (Hardy et al. 2001; Hardy 2007; Sabet et al. 2008). Injury prediction capabilities will continue to increase as brain models are improved and validated against more

experimental data. FE models also allow simulation and evaluation of injury mitigation and prevention systems, such as seat belts and air bags. As prediction capacity improves, simulation of injury scenarios, such as motor vehicle crashes, will become more accurate and enhance the study of brain injuries. This will advance our knowledge of injury mechanisms and the effectiveness of prevention and mitigation systems.

ACKNOWLEDGEMENTS

Funding for this project is provided by the National Institutes of Health (R01 NS082453). All simulations were run on the DEAC Cluster at Wake Forest University. The authors would like to thank the ANSIR lab for providing the ICBM labelmaps, Elizabeth Lillie for her work on the MATLAB code to produce the ABM from the labelmaps, and the THUMS and GHBMC teams at Wake Forest University for providing the respective head models.

REFERENCES

Al-Bsharat AS, Hardy WN, Yang KH, Khalil TB, Tashman S, King AI. Brain/skull relative displacement magnitude due to blunt head impacts: new experimental data and model. Stapp Car Crash J. 1999;43(2):321–32.

Bandak FA, Eppinger RH. A three-dimensional finite element analysis of the human brain under combined rotational and translational accelerations. SAE Technical Paper; 1994. Report No.: 0148–7191.

Bandak F, Zhang A, Tannous R, DiMasi F, Masiello P, Eppinger RH. Simon: a simulated injury monitor; application to head injury assessment. National Highway Traffic Safety Administration; 2001. p. 7–p.

Chafi MS, Dirisala V, Karami G, Ziejewski M. A finite element method parametric study of the dynamic response of the human brain with different cerebrospinal fluid constitutive properties. Proc Inst Mech Eng [H]. 2009 Nov;223(8):1003–19.

Chatelin S, Constantinesco A, Willinger R. Fifty years of brain tissue mechanical testing: from in vitro to in vivo investigations. Biorheology. 2010;47(5):255–76.

Clemente CD. Gray's Anatomy, 30th American Edition of the Anatomy of the Human Body by Henry Gray, 1825-1861. ed. (1985). PA: Lea & Febiger; 1985.

Coronado VG, Xu L, Basavaraju SV, McGuire LC, Wald MM, Faul MD, et al. Surveillance for Traumatic Brain Injury-Related Deaths - United States, 1997–2007. Morb Mortal Wkly Rep. 2011;60(5):1–32.

Deck C, Willinger R. The current state of the human head finite element modelling. Int J Veh Saf. 2009;4(2):85–112.

DiMasi FP, Eppinger RH, Bandak FA. Computational analysis of head impact response under car crash loadings. 39th Stapp Car Crash Conf. Society of Automotive Engineers; 1995. p. 425–38.

Donnelly B, Morgan RM, Eppinger RH. Durability, repeatability and reproducibility of the NHTSA side impact dummy. International Research Council on Biomechanics of Injury; 1983. p. 299–310.

Faul M, Xu L, Wald MM, Coronado VG. Traumatic Brain Injury in the United States: Emergency Department Visits, Hospitalizations and Deaths 2002-2006. Cent Dis Control Prev Natl Cent Inj Prev Control. 2010;

Gehre C, Gades H, Wernicke P. Objective Rating of Signals Using Test and Simulation Responses. Pap Present 21st ESV Conf. 2009 Jun 15;

Giordano C, Kleiven S. Evaluation of Axonal Strain as a Predictor for Mild Traumatic Brain Injuries Using Finite Element Modeling. Stapp Car Crash J. 2014;58:29.

Gross AG. Impact thresholds of brain concussion. J Aviat Med. 1958;29(10):725–32.

Hardy WN. Response of the Human Cadaver Head to Impact. [Detroit, MI]: Wayne State University; 2007.

Hardy WN, Foster CD, Mason MJ, Yang KH, King AI, Tashman S. Investigation of Head Injury Mechanisms Using Neutral Density Technology and High-Speed Biplanar X-ray. Stapp Car Crash J. 2001 Nov;45:337–68.

Hodgson V, Thomas LM, Gurdjian E, Fernando O, Greenberg S, Chason J. Advances in understanding of experimental concussion mechanisms. SAE Technical Paper; 1969.

Holbourn A. Mechanics of head injuries. The Lancet. 1943;242(6267):438–41.

Horgan TJ, Gilchrist MD. Influence of FE model variability in predicting brain motion and intracranial pressure changes in head impact simulations. Int J Crashworthiness. 2004;9(4):401–18.

Ji S, Ghadyani H, Bolander RP, Beckwith JG, Ford JC, McAllister TW, et al. Parametric comparisons of intracranial mechanical responses from three validated finite element models of the human head. Ann Biomed Eng. 2014a Jan;42(1):11–24.

Ji S, Zhao W, Ford JC, Beckwith JG, Bolander RP, Greenwald RM, et al. Group-wise evaluation and comparison of white matter fiber strain and maximum principal strain in sports-related concussion. J Neurotrauma. 2014b;(ja).

Ji S, Zhao W, Li Z, McAllister TW. Head impact accelerations for brain strain-related responses in contact sports: a model-based investigation. Biomech Model Mechanobiol. 2014c Oct;13(5):1121–36.

Jiroušek O, Jíra J, Jírová J, Micka M. Finite element model of human skull used for head injury criteria assessment. Springer; 2005. p. 459–67.

Jovanovski J. Crash data analysis and model validation using correlation techniques. SAE Technical Paper; 1981. Report No.: 0148–7191.

Kimpara H, Nakahira Y, Iwamoto M, Miki K, Ichihara K, Kawano S, et al. Investigation of anteroposterior head-neck responses during severe frontal impacts using a brain-spinal cord complex FE model. Stapp Car Crash J. 2006;50:509–44.

King AI, Yang KH, Zhang L, Hardy W, Viano DC. Is head injury caused by linear or angular acceleration. 2003. p. 1–12.

Kleiven. Evaluation of head injury criteria using a finite element model validated against experiments on localized brain motion, intracerebral acceleration, and intracranial pressure. Int J Crashworthiness. 2006;11(1):65–79.

Kleiven S. Predictors for traumatic brain injuries evaluated through accident reconstructions. Stapp Car Crash J. 2007 Oct;51:81–114.

Kleiven S, Hardy WN. Correlation of an FE Model of the Human Head with Local Brain Motion--Consequences for Injury Prediction. Stapp Car Crash J. 2002 Nov;46:123–44.

Kleiven S, von Holst H. Consequences of head size following trauma to the human head. J Biomech. 2002 Feb;35(2):153–60.

Mao H, Zhang L, Jiang B, Genthikatti VV, Jin X, Zhu F, et al. Development of a finite element human head model partially validated with thirty five experimental cases. J Biomech Eng. 2013 Nov;135(11):111002.

Mao H, Zhang L, Yang KH, King AI. Application of a finite element model of the brain to study traumatic brain injury mechanisms in the rat. Stapp Car Crash J. 2006 Nov;50:583–600.

Mazziotta J, Toga A, Evans A, Fox P, Lancaster J, Zilles K, et al. A probabilistic atlas and reference system for the human brain: International Consortium for Brain Mapping (ICBM). Philos Trans R Soc Lond B Biol Sci. 2001 Aug 29;356(1412):1293–322.

Mazziotta JC, Toga AW, Evans A, Fox P, Lancaster J. A probabilistic atlas of the human brain: theory and rationale for its development. The International Consortium for Brain Mapping (ICBM). NeuroImage. 1995 Jun;2(2):89–101.

Mendis K, Stalnaker R, Advani S. A constitutive relationship for large deformation finite element modeling of brain tissue. J Biomech Eng. 1995;117(3):279–85.

Miller LE, Urban JE, Stitzel JD. Development and validation of an atlas-based finite element brain model. Biomech Model Mechanobiol. 2016;1–14.

Nahum AM, Smith R, Ward CC. Intracranial pressure dynamics during head impact. SAE Technical Paper; 1977.

Pudenz RH, Shelden CH. The lucite calvarium; a method for direct observation of the brain; cranial trauma and brain movement. J Neurosurg. 1946 Nov;3(6):487–505.

Sabet AA, Christoforou E, Zatlin B, Genin GM, Bayly PV. Deformation of the human brain induced by mild angular head acceleration. J Biomech. 2008;41(2):307–15.

Takhounts EG, Eppinger RH, Campbell JQ, Tannous RE, Power ED, Shook LS. On the Development of the SIMon Finite Element Head Model. Stapp Car Crash J. 2003 Oct;47:107–33.

Takhounts EG, Ridella SA, Hasija V, Tannous RE, Campbell JQ, Malone D, et al. Investigation of traumatic brain injuries using the next generation of simulated injury monitor (SIMon) finite element head model. Stapp Car Crash J. 2008 Nov;52:1–31.

Trosseille X Domont, A.Guillon, F.Lavaste, F.Tarriere, C. Development of a F.E.M. of the human head according to a specific test protocol. 1992.

Tse KM, Tan LB, Lee SJ, Lim SP, Lee HP. Development and validation of two subject-specific finite element models of human head against three cadaveric experiments. Int J Numer Methods Biomed Eng. 2014;30(3):397–415.

Vavalle NA, Jelen BC, Moreno DP, Stitzel JD, Gayzik FS. An Evaluation of Objective Rating Methods for Full-Body Finite Element Model Comparison to PMHS Tests. Traffic Inj Prev. 2013 Jan 1;14(sup1):S87–94.

Yu H, Medri M, Zhou Q, DiMasi F, Bandak F. Head–neck finite element model of the crash test dummy THOR. Int J Crashworthiness. 2004;9(2):175–86.

Zhang L, Yang KH, Dwarampudi R, Omori K, Li T, Chang K, et al. Recent advances in brain injury research: a new human head model development and validation. Stapp Car Crash J. 2001a Nov;45:369–94.

Zhang L, Yang KH, King AI. Comparison of Brain Responses Between Frontal and Lateral Impacts by Finite Element Modeling. J Neurotrauma. 2001b;18(1):21–30.

APPENDIX

Table 3: Comparison of brain FE models

	#elements/ #nodes	Mass (kg)	Brain Material Model	Brain Shear Parameters	Validation	
					ICP	Local Displacements
ABM	2,000,000/ 2,000,000	1.74†	Viscoelastic	G_0=5.16 kPa G_∞=1.86 kPa β=67.58 s^{-1}	--	• C755-T2 • C383-T1 • C291-T1
SIMon	46,000/ 42,500	1.10†	Viscoelastic	G_0=1.66 kPa G_∞=0.93 kPa β=16.95 s^{-1}	• Exp. 37 • Exp. MS 428-2	• C755-T2 • C383-T1 • C291-T1
GHBMC	230,000/ 190,000	1.19†	Viscoelastic	**Gray:** G_0=6 kPa G_∞=1.2 kPa β=12.5 s^{-1} **White:** G_0=7.5 kPa G_∞=1.5 kPa β=12.5 s^{-1}	• Exp. 37 • Exp. MS 428-2	• C383-T3 • C755-T2 • C241-T1 • C241-T6 • C380-T4 • C393-T4 • C380-T3 • C380-T5
THUMS	62,000/ 38,000	1.08†	Viscoelastic	**Gray:** G_0=10 kPa G_∞=5 kPa β=0.06 s^{-1} **White:** G_0=12.5 kPa G_∞=6.13 kPa β=0.06 s^{-1}	• Exp. 37 • Exp. MS 428-2	• C383-T1 • C755-T2
KTH (2006)	18,000/ 20,000	4.44*	Hyperelastic (Mooney-Rivlin)	G_1=1628 Pa, β_1=125 s^{-1} G_2=930 Pa, β_2=6.67 s^{-1}	• Exp. 37 • Exp. MS 428-2	• C383-T1 • C383-T2 • C383-T4 • C755-T2 • C291-T1 • C380-T4 • C380-T5 • C288-T3
KTH	21,000/ 17,000	4.52*	Hyperelastic (Ogden)	μ_1=53.8 Pa, α_1=10.1 μ_2=-120.4 Pa, α_2=-12.9 G_1=320 kPa, β_1=10^6 s^{-1} G_2=78 kPa, β_2=10^5 s^{-1} G_3=6.2 kPa, β_3=10^4 s^{-1} G_4=8 kPa, β_4=10^3 s^{-1} G_5=0.1 kPa, β_5=10^2 s^{-1} G_6=3 kPa, β_6=10^1 s^{-1}	• Exp. 37 • Exp. MS 428-2	• C383-T1 • C383-T2 • C383-T4 • C755-T2 • C291-T1 • C380-T4 • C380-T5 • C288-T3
DHIM	115,000/ 101,000	4.56*	Hyperelastic (Ogden)	μ_1=271.7 Pa, α_1=10.1 μ_2=776.6 Pa, α_2=-12.9 g_1=7.69e-1, τ_1=1e-6 s g_2=1.86e-1, τ_2=1e-5 s g_3=1.48e-2, τ_3=1e-4 s g_4=1.90e-2, τ_4=1e-3 s g_5=2.56e-3, τ_5=1e-2 s g_6=7.04e-3, τ_6=1e-1 s	• Exp. 37 • Exp. MS 428-2	• C383-T1 • C755-T2 • C393-T4

†brain mass
*total model mass